A Novel Preamble Design for 5G Enabled LEO Non-Terrestrial Networks

1st Hua-Min Chen
Faculty of Information Technology
Beijing University of Technology,
Beijing, P.R.China.
chenhuamin@bjut.edu.cn

2nd Peng Wang
Beijing Institute of Remote Sensing Equipment
Beijing, P.R.China
wp_fuyao@163.com

3rd Sijia Li
Beijing-Dublin International College
Beijing University of Technology,
Beijing, P.R.China.
lisijia0226@emails.bjut.edu.cn

4th Shaofu Lin
Faculty of Information Technology
Beijing University of Technology,
Beijing, P.R.China.
linshaofu@bjut.edu.cn

5th Zhuwei Wang
Faculty of Information Technology
Beijing University of Technology,
Beijing, P.R.China.
wangzhuwei@bjut.edu.cn

6th Chao Fang
Faculty of Information Technology
Beijing University of Technology,
Beijing, P.R.China.
fangchao.bupt@gmail.com

GLOBECOM 2022 - 2022 IEEE Global Communications Conference | 978-1-6654-3540-6/22/$31.00 ©2022 IEEE | DOI: 10.1109/GLOBECOM48099.2022.10001203

***Abstract*—A novel random access (RA) preamble format is proposed in this paper to support fifth generation new ratio (5G NR) enabled satellite system, which is a low earth orbiting (LEO) based non-terrestrial network (NTN). Considering a fact that traditional design of RA preamble can not meet the link budget due to a long distance between the satellite and terminal on the earth, and also will cause a wrong or failure detection of PRACH, or wrong timing estimation for uplink synchronization. The frequency offset under the large relative moving speed between the satellite and the terminal will also increase the failure detection of PRACH (physical random access channel). Therefore, a novel RA preamble format, i.e., a Zadoff-Chu (ZC) sequence with multiple lengths, are designed. To reduce the ambiguous estimation of RA preamble, a symmetric transmission of the proposed preamble is analyzed. Further, two detection algorithms (Algorithm 1 and Algorithm 2) are proposed to detect PRACH. Simulation results validate that the proposed RA preamble can meet the LEO based NTN performance requirements. According to simulation results, it can be proved that Algorithm 2 is more robust, considering timing error and frequency offset.**

***Index Terms*—RA preamble, 5G NR, NTN, LEO, frequency offset, timing delay**

I. Introduction

Satellite network is a significant solution to provide communication services to mobile users in sparsely-populated regions, in emergency areas, on planes, trains, and ships. Especially for the rescue and disaster relief, military, aeronautical, maritime, etc, satellite communication plays an important role [1]. It is predictable that satellite communication will become an indispensable component of the incoming fifth or sixth generation (5G/6G) global networks, and ongoing activities are undertaken by 3rd generation partnership project (3GPP) [2]- [5]. When to design the satellite systems, one natural way is to maximize the utilization of current specified technologies with the terrestrial systems, so as to keep implementation costs to a minimum, satisfying NTN requirements, while simplifying interactive procedures and reducing time period.

As an important part for data service, random access (RA) helps to establish the uplink (UL) connection between the user equipment (UE) and next generation NodeB (gNB) or base station (BS), and there have been some related works about RA preamble design and detection [6]- [9]. However, due to the movement of the NTN platform and long prorogation distance between the satellite and UE, special attention is paid to RA preamble design with the consideration of higher doppler shift, larger link budget and timing advance (TA) [10]- [12]. Taking an example of a low earth orbiting (LEO) based NTN system at the height of 1200km and working at Ka band, a time-varying doppler shift can be as large as 21 ppm (around 630 kHz at 30 GHz carrier frequency), and the maximum propagation delay is up to 10.5ms [3]. Then, it's required that the UE must acquire time and frequency synchronization in the downlink (DL), otherwise there will be a huge burden for NTN gNB or the performance of successful access degrades sharply.

There are some works on RA preamble design for the satellite networks. Regarding the increase prorogation delay over the NTN channel, one way is to add a TA at UE before transmitting RA preamble [13]- [14]. The main basic consideration for these works is a global navigation satellite system (GNSS) receiver can be used in order to estimate the location of the satellite and UE, so as to derive the TA required. However, the GNSS signals are weak, not ubiquitous, and susceptible to interference and spoofing [15]. Then, it's possible that the timing synchronization fails if an UE is out of GNSS coverage. In [16] and [17] , a fixed TA is applied according to the center of the satellite antenna footprint, and the synchronization gap is handled by the satellite. Some possible solutions are also investigated by 3GPP [3], and it

This paper was supported by the National Key Research and Development Program of China (2020YFF0305401).

can be concluded that TA estimation and compensation at NTN BS are required. Correspondingly, RA preamble design should consider the time-varying synchronization shift.

Moreover, it's hard to distinguish doppler shift due to the high speed movement and carrier frequency offset (CFO) caused by a crystal oscillator, though there are many researches on frequency offset estimation for orthogonal frequency division multiplexing (OFDM) system [19] [20] and also some work about doppler shift measurement [21] [22]. According to work in [23] [24], there are several peaks in the ambiguity function of Zadoff-Chu (ZC) sequences, leading to many timing and Doppler ambiguities. It will be necessary to separate delay and frequency shift, and it's difficult to distinguish these two effects by observing the composite cyclic shift.

Considering the expense, size and power restriction of a satellite, a simplified RA preamble algorithm is preferred, which requires the design of RA preamble for NTN is robust enough. In this paper, we consider a new RA preamble format, including cyclic prefix (CP) and guard period (GT). Further, the proposed new format comprises two parts for TA and frequency offset measurement, respectively. In the rest of this paper, we first give a novel design of RA preamble for LEO NTN in section II, wherein the system model is briefly described and corresponding link budget is discussed according to the system parameters. Simulation results are presented in III. Finally, section IV concludes the paper.

II. Design of RA Preamble for LEO NTN

For easy reading, some symbols, abbreviations and system parameters are summarized in Table I. Fig. 1 gives an illustration of stand alone 5G enabled LEO NTN system working in Ka band and with a height of 1100km, and corresponding link budget at the direction of maximal elevation angle and the center is summarized in Table II, according to the link budget expression in [3]. Obviously, current 5G design for RA preamble [25] can not work under such low SNR environment.

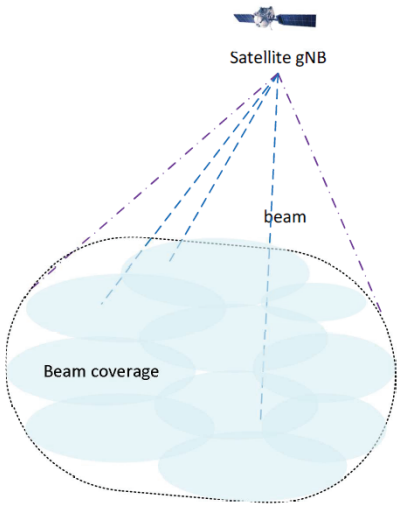

Fig. 1. Illustration of a 5G enabled NTN system

TABLE I
Notation Explanation

Parameter	Value & Explanation
System bandwidth	400MHz
Frequency range	30GHz
Elevation angle	$\pm 55°$
LEO NTN speed	$\sim 7\text{km/s}$
UL EIRP	$\geq 40\text{dBW}$
UL G/T	$\geq 1.87\text{dB/K}$
N_{R}	number of receiver antenna
N_{SW}	number of PRACH search window
N_{seq}	sequence length of a single RA preamble in the unit of sample
N_{CP}	CP length of a single RA preamble format in the unit of sample
N_{GT}	GT length of a single RA preamble format in the unit of sample
N_{rep}	RA preamble repetition number
N_{FFT}	FFT/IFFT point number
T_{CP}	time duration of CP length in the unit of us
T_{GT}	time duration of GT length in the unit of us
κ	over sampling rate constant as 64
μ	subcarrier spacing configuration $15 \cdot 2^{-\mu}\text{KHz}$
EIRP	Equivalent Isotropic Radiated Power
G/T	Antenna gain to noise temperature
PRB	Physical resource block
SCS	subcarrier spacing
FFT/IFFT	Fast Fourier Transform/Inverse Fast Fourier Transform

A. Proposed RA Preamble for LEO NTN

In general, a RA preamble comprises a cyclic prefix (CP), a ZC sequence (SEQ) and a guard time (GT), and their durations are denoted as N_{CP}, N_{seq} and N_{GT} in the unit of sample number. Further, the sequence can be repeatedly transmitted by N_{rep} to guarantee the coverage and performance, as shown in Fig. 2. In this figure, N_u stands for the length of a valid RA preamble. Under the NR design of RA preamble, the PRACH sequence $x_{u,v}$ can be expressed as [26]

$$\begin{cases} x_{u,v}(n) = x_u\left((n + F(v)) \bmod N_{\text{seq}}\right) \\ x_u(i) = e^{-j\frac{\pi u i(i+1)}{N_{\text{seq}}}}, i = 0, 1, ..., N_{\text{seq}} - 1, \end{cases} \quad (1)$$

where i is the root sequence index, u is associated with a unique inverse modulo N_{seq} which is a prime number for a ZC sequence, v is the cyclic shift. One thing to be noted is the sequence length N_{seq} is a prime number for a ZC sequence.

For RA preamble design, CP is used to suppress inter symbol interference (ISI) caused by round trip time (RTT) and delay spread. By considering the fact that the maximum delay

TABLE II
UL LINK BUDGET

Channel Type	Center	Maximal Elevation Angle
Channel Bandwidth (MHz)	350MHz	350MHz
PRB Number	243	243
subcarrier spacing(KHz)	120	120
Carrier Frequency(GHz)	30	30
Elevation angle (°)	0	60
EIRP (dBW)	40.00	33.00
Tx Beam loss (dB)	0	7
Free space path loss (dB)	182.81	188.82
Atmospheric loss (dB)	0.50	0.50
G/T (dB/K)	1.87	1.87
Receiver beam loss (dB)	0	5
received SNR(dB)	6.22	-10.82

TABLE III
RA PREAMBLE FORMATS FOR LEO NTN

Format	SCS	N_{seq}	N_u	N_{CP}, N_{GT}
F0	30KHz	251	$12 \cdot 2048\kappa \cdot 2^{-\mu}$	$2048\kappa \cdot 2^{-\mu}$
F1	30KHz	251	$28 \cdot 2048\kappa \cdot 2^{-\mu}$	$2048\kappa \cdot 2^{-\mu}$
F2	60KHz	251	$12 \cdot 2048\kappa \cdot 2^{-\mu}$	$2048\kappa \cdot 2^{-\mu}$
F3	60KHz	251	$28 \cdot 2048\kappa \cdot 2^{-\mu}$	$2048\kappa \cdot 2^{-\mu}$
F4	15KHz	509	$12 \cdot 2048\kappa \cdot 2^{-\mu}$	$2048\kappa \cdot 2^{-\mu}$
F5	15KHz	509	$28 \cdot 2048\kappa \cdot 2^{-\mu}$	$2048\kappa \cdot 2^{-\mu}$
F6	60KHz	509	$12 \cdot 2048\kappa \cdot 2^{-\mu}$	$2048\kappa \cdot 2^{-\mu}$
F7	60KHz	509	$28 \cdot 2048\kappa \cdot 2^{-\mu}$	$2048\kappa \cdot 2^{-\mu}$
F8	15KHz	1021	$5 \cdot 2048\kappa \cdot 2^{-\mu}$	$2048\kappa \cdot 2^{-\mu}$
F9	15KHz	1021	$12 \cdot 2048\kappa \cdot 2^{-\mu}$	$2048\kappa \cdot 2^{-\mu}$
F10	30KHz	1021	$5 \cdot 2048\kappa \cdot 2^{-\mu}$	$2048\kappa \cdot 2^{-\mu}$
F11	30KHz	1021	$12 \cdot 2048\kappa \cdot 2^{-\mu}$	$2048\kappa \cdot 2^{-\mu}$

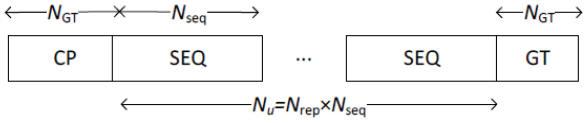

Fig. 2. Illustration of a general RA preamble

spread is much smaller than RTT in satellite communication, it's reasonable to only consider the time uncertainty and determines as $T_{\text{CP}} = T_{\text{GT}} = T_{\text{RTT}}$, where T_{CP}, T_{GT} and T_{RTT} corresponds to time duration of CP, GT and RTT with a unit of us. The overhead of CP and GT will result a large resource waste, if CP and GT is designed to compensate RTT which can be up to around 20ms for a LEO NTN system.

In this paper, a LEO NTN system with a sampling rate as 491.52GHz and $N_{\text{FFT}} = 4096$ is considered. To facilitate signal processing, CP and GT length is designed to be rational to N_{FFT} as $\eta \times N_{\text{FFT}}$. Further, the generated RA preamble is also over sampled as long as N_{FFT}, then the time duration of one RA preamble can align with the OFDM or slot boundary. Then, the overall RA preamble duration in sample can be obtained as

$$\begin{aligned} L_{\text{RA}} &= N_{\text{CP}} + N_{\text{GT}} + N_u \\ &= 2\eta N_{\text{FFT}}\kappa 2^{-\mu} + N_{\text{rep}}\eta N_{\text{FFT}}\kappa 2^{-\mu}. \end{aligned} \tag{2}$$

For example, considering a 30KHz SCS for RA preamble transmission within a 120KHz system SCS, a RA preamble with $N_{\text{CP}} = N_{\text{GT}} = 4096\kappa \cdot 2^{-1}$ and $N_{\text{rep}} = 12$ could will occupy 8 slots equivalent to around 1ms. Under the restriction of signal processing and delay, this paper proposes to have $\eta = 1/2$ to have a unified design.

Smaller SCS is sensitive to large frequency offset in a NTN scenario. Compare to original 1.25KHz and 2.5KHz for long RA preamble [26], it's proposed to adopt 15KHz, 30KHz, 60KHz and 120KHz for new designed RA preamble to support different types of UEs, such as planes, trains, and so on. One basic principle is longer sequence length and smaller SCS to extend the data service provided by LEO NTNs. Considering the signal processing complexity and hardware development for NTN, this paper consider a different length of sequence length to simplify FFT/IFFT operation. That is to say the sequence length is a prime number and is as close as $2^{N_{\text{FFT}}}$, where N_{FFT} is the number of FFT/IFFT operation. Therefore, new sequence length N_{seq} is $\{251, 509, 1021\}$.

Table III summarizes possible RA preamble formats for the LEO NTN system, based on above discussion.

B. RA Transmission for LEO NTN

Fig. 3 gives the detection flow of PRACH. According to previous work in [23] [24], there is timing and doppler ambiguities in RA preamble. The ambiguous of PRACH peak power will increase under larger doppler shift and time delay, as shown in Fig. 4. The receiver aims to estimate delay and frequency offset by cross correlating the received signal with its reference copy of the transmitted signal. The correlation is performed at multiple hypotheses of frequency offsets that are on the step size of 1.25 kHz. The sampling rate is 30.72 MHz. The cross correlation results are normalized power by the maximum correlation value. It is clear that multiple correlation peaks of the similar height are observed. This implies that it is impossible to separate the effects of delay and frequency offset in PRACH in the presence of both large timing and frequency uncertainties, leading to difficulties in timing estimate at the gNB and mis-detection of random access preambles.

Let Δf be the frequency offset between transmitted and received signals, and SCS stands for the subcarrier spacing in the unit of KHz, we can have the peak number as

$$\Delta k = \Delta f / \text{SCS}, \tag{3}$$

Then, both delay and frequency shift cause cyclic shift in the received ZC sequences, resulting in a composite cyclic shift

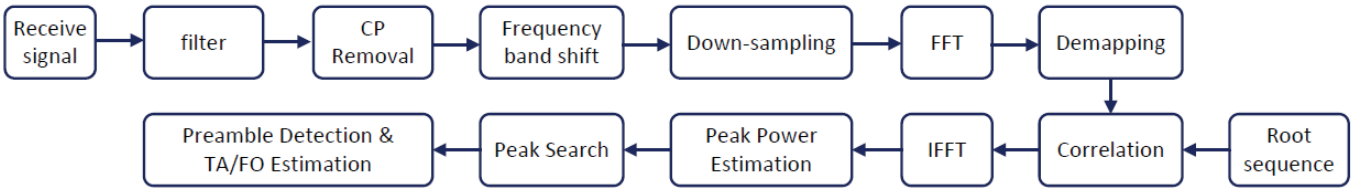

Fig. 3. Detection flow of RA preamble

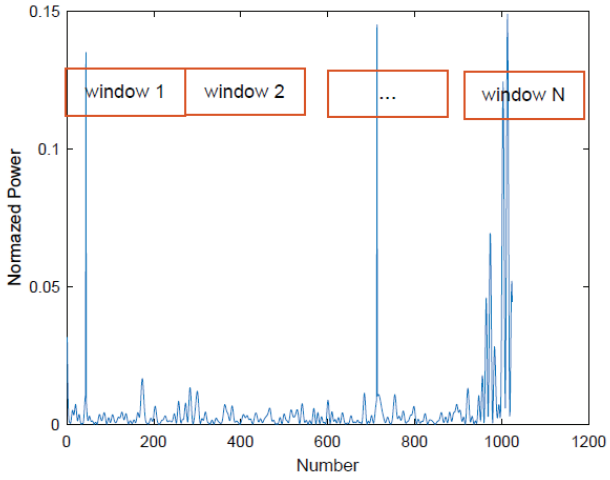

Fig. 4. Illustration of PRACH search window

from which the effect of delay cannot be separated from the effect of frequency shift.

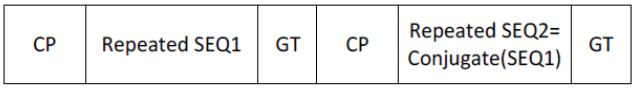

Fig. 5. Illustration of a proposed RA preamble transmission

Therfore, if a transmitter sends two signals based on two ZC sequences $s1$ and $s2$ (that have different properties), the receiver can resolve the timing and frequency offset ambiguities by processing the two received signals. Note that for simplicity we assume that the frequency offset is an integer multiple of the subcarrier spacing. For more general case, it can be shown that the squared autocorrelation of ZC sequence is given by

$$|\Re\left(\Delta n, \Delta f\right)|^2 = \left|\mathrm{sinc}\left(\frac{\Delta f}{\mathrm{SCS}} - u\Delta n\right)\right|^2, \tag{4}$$

where $\Re$ denotes the autocorrelation, Δn corresponds to TA. Then, time delay Δn and frequency offset Δf can be estimated by processing the two received $s1$ and $s2$ with roots u and $-u$ respectively. Note that $s2$ with a root $-u$ is a conjugate of $s1$. Fig. 5 shows the structure of such proposed RA transmission. Under such design, two identical branches of the detection flow in Fig. 3 is needed.

C. Peak Power Search Algorithm 1

As shown in Fig. 4, each search window corresponds to a preamble index. Algorithm 1 with two thresholds $Thr_{1\mathrm{A}}$ and $Thr_{1\mathrm{B}}$ is designed as following.

Firstly, calculate the average power delayed power (PDP) for each root value of each occasion as

$$Thr_{1\mathrm{A}} = \frac{\partial}{N_{\mathrm{FFT}}} \sum_{n=1}^{N_{\mathrm{FFT}}} P_u\left(n\right), \tag{5}$$

where $P_u\left(n\right)$ denotes the IFFT output of correlation operation between received PRACH signal and the root sequence under u, ∂ is a scaling factor to reduce the false alarm detection and obtained by a chi-square distribution [27]

$$\begin{cases} \partial = G_{soft}^{-1}\left[\left(1-P_{\mathrm{FA}}\right)^{\frac{1}{N_{\mathrm{FFT}}}}\right] \Big| P_{\mathrm{FA}} = 0.1\% \\ G_{soft}\left(x\right) = F_{\chi^2}\left(x, 2N_{\mathrm{R}}N_{\mathrm{rep}}, 0\right). \end{cases} \tag{6}$$

Obviously, it can be noticed that value of ∂ changes with the PRACH format listed in Table III, wherein N_u is different and N_{FFT} changes with N_{seq}.

Then, obtain a peak threshold $Thr_{1\mathrm{B}}$ through averaging the power values larger than $Thr_{1\mathrm{A}}$ in each window corresponding to a single u by

$$Thr_{1\mathrm{B}} = \frac{1}{N_s} \sum_{n=1}^{N_{\mathrm{FFT}}} \left\{P_u\left(n\right) > Thr_{1\mathrm{A}}\right\}, \tag{7}$$

where N_s means the sample number of $\{P_u\left(n\right) > Thr_{1\mathrm{A}}\}$.

Finally, one or more u can be obtained if the maximal PDP value in each window is larger than $Thr_{1\mathrm{B}}$.

D. Peak Power Search Algorithm 2

Under Algorithm 1, some potential peaks may still exist due to the randomization of background noise and change of channel status. Further, the randomization transmission of PRACH, especially in case of larger UE density, the detection accuracy will be affected, if the gap of different shift v is not large enough. As shown in Fig. 6, in one window, multiple shift values corresponding to different PRACH sequence $x_{u,v}$ will be detected, in case of same timing Δ/N_{FFT}. Further, under different timing (0.1 and 0.2), two different v is detected in two different windows corresponding to different u at the same time.

Moreover, under Algorithm 1, it will be likely to remove the potential UE peaks, but not the peak side lobes, if we simply eliminate just the peak sample from each search window.

Furthermore, it's also risk removing some high value noise correlation peaks, which is not desirable as this leads to under estimation of background correlation level, when no UE is transmitting in a certain correlation window.

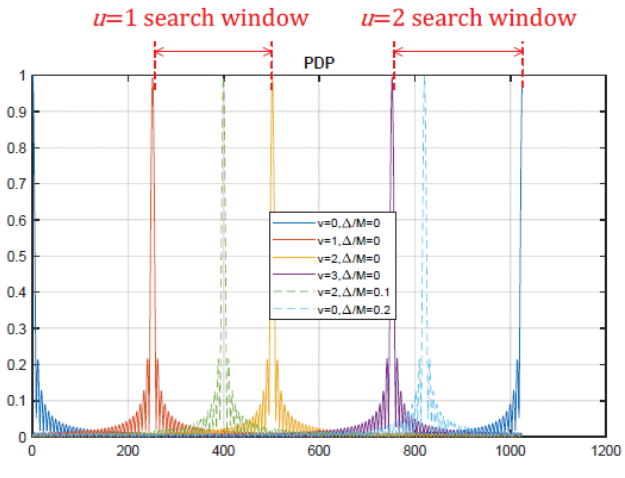

Fig. 6. Illustration of peak power ambiguity under Algorithm 1

Therefore, a new method is proposed to further reduce the ambiguity of multiple peaks and false alarm during detection. The main different from Algorithm 1 is some samples around the peak power are also removed. Then, the set size of $\{P_u(n) > Thr_{1A}\}$ in (7) will be restricted. For easy description, let $\Im = \{k_1, \ldots, k_{N_{SW}}\}$ denotes peak index of the maximal peak values in each search window. Then, $\Im$ is extended by removing N_{rm} samples around each peak as

$$\begin{aligned}\Im_{ext} = \{&k_1 - N_{rm}, k_1 - N_{rm} + 1, k_1 + N_{rm}, \ldots, \\ &k_{N_{SW}} - N_{rm}, \ldots, k_{N_{SW}} + N_{rm}\}\end{aligned} \tag{8}$$

Then, (5) can be revised and a new threshold Thr_{2A} can be calculated as

$$Thr_{2A} = \frac{\partial}{N_{FFT} - |\Im_{ext}|} \left(\sum_{n=1}^{N_{FFT}} P_u(n) - \sum_{j=1}^{|\Im_{ext}|} P_u(j) \,|\, j \in \Im_{ext} \right) \tag{9}$$

where $|\Im_{ext}|$ is the sample number of $\Im_{ext}$.

III. Simulation Results

According to the listed parameters in Table I and II, and the proposed RA preamble in II, this section presents the evaluation results. For performance comparison, 5G RA preamble format B4 is selected as a benchmark, with a preamble length as 139 and repetition time as 12, and 93due to higher SCS, longer CP length and larger repetition number. UE velocity is 0km/h and 1000km/h according to the assumption in [3].

First of all, the detection rate is compared under proposed F3 and 5G RA preamble format B4 with RA SCS as 60KHz in Fig. 7. The reason to choose B4 is the only legacy format supporting 12 repetitions. Further, the preamble duration of B4 is $12 \cdot 2048 \cdot \kappa \cdot 2^{-mu}$, which is similar to our proposed preamble. The residual frequency offset is assumed to be 100KHz. It can be observed that the proposed format F3 with a larger CP outperforms B4 by a 0.8dB at 1% missing rate, when the UE velocity is 0km/h. Increasing UE velocity to 1000km/h which results in a larger frequency offset, the performance of both formats decrease. Specifically, the performance of proposed F3 decreases by around 1.5dB, while the gap is 4dB for B4. The possible reason for such result is there are more ambiguous power peaks for legacy B4 under a large frequency offset, while a symmetric transmission of a sequence and a conjugate one helps to diminish such ambiguity.

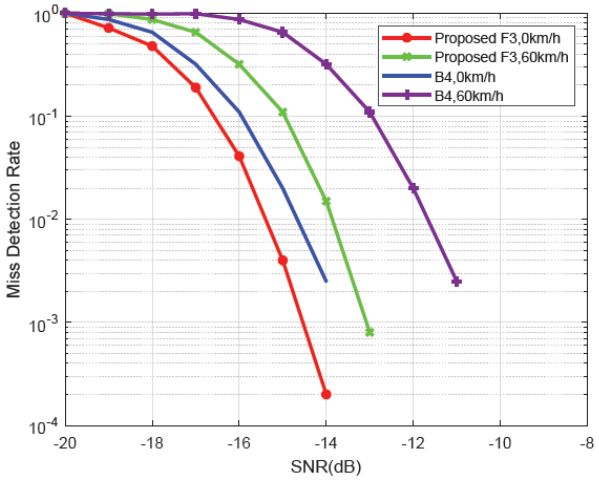

Fig. 7. Miss detection rate of short RA preamble detection ($N_{seq} = 251$, RA SCS=60KHz)

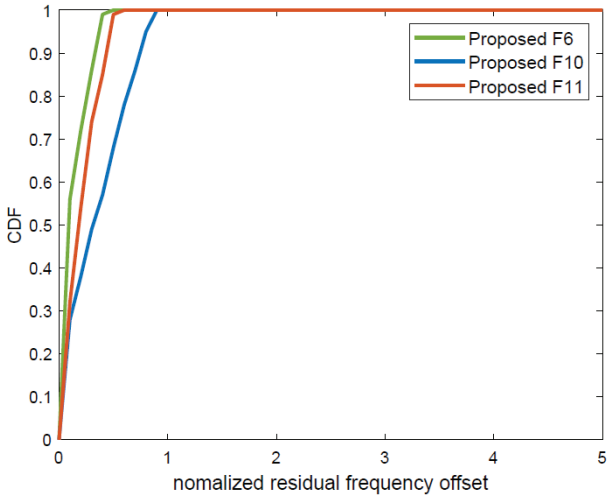

Fig. 8. CDF of residual frequency offset

The CDFs of normalized residual frequency offset and residual timing offset at the SNR point corresponding to 99% preamble detection rate is illustrated in Fig 8. Obviously, it

can be observed that the normalized residual frequency offset does not exceed 1 SCS for all considered formats. In case of F10 and F11 with 30KHz SCS, F6 has better performance due to larger SCS with a better capability for frequency offset estimation and compensation. Different from F10 with only 5 repetitions, F11 has a little better gain under 12 repetitions.

Table IV and Table V compare the performance between Algorithm 1 and Algorithm 2. From Table IV, it can be observed that Algorithm 2 has lower SNR range for 0.1% false alarm rate. Considering the link budget in Table II, there is a risk for Algorithm 1 under 15KHz frequency offset. Such result aligns with the analysis of Algorithm 2 wherein more possible peak values are removed for threshold calculation that is independent of SNR and the presence or absence of UE signals.

Regarding the timing error during PRACH detection, Table V summarizes format F0 and F5. As analyzed in section II-D, some high value noise correlation peaks can be eliminated, especially under different channel conditions, and the corresponding timing can be more accurate.

TABLE IV
0.1% FALSE ALARM COMPARISON BETWEEN ALGORITHM 1 AND ALGORITHM 2 UNDER FORMAT F2

Frequency offset	Algorithm 1	Algorithm 2
0Hz	-13.5dB	-18.5dB
4KHz	-15dB	-18dB
15KHz	-8dB	-12dB

TABLE V
TIME ERROR COMPARISON BETWEEN ALGORITHM 1 AND ALGORITHM 2

Format	Algorithm 1	Algorithm 2
F0	1.77us	0.26us
F5	2.03us	0.52us

IV. CONCLUSION

This paper addresses the issue of RA preamble design in the environment of mobile satellite communications. Considering a fact that traditional design of RA preamble can not meet the link budget due to a long distance between the satellite and terminal on the earth, a link budget analysis is provided in the paper as a baseline. Further, a large timing will cause a wrong or failure detection of PRACH, or wrong timing estimation for uplink synchronization. The frequency offset under the large relative moving speed between the satellite and the terminal will also increase the failure detection of PRACH. Therefore, a novel RA preamble format supporting short and long preamble sequence is designed for a 5G enabled LEO NTN.

To reduce the ambiguous estimation of RA preamble, a symmetric transmission of the proposed preamble is analyzed. It means that a pair of a preamble and a conjugate copy of the preamble is transmitted at each RA occasion. Then, one is for timing and the other can be used for frequency offset estimation under a more finer timing estimation. Two detection algorithms are analyzed to improve PRACH detection performance. Simulation results have demonstrated the performance improvement in terms of success access rate and residual frequency offset.

REFERENCES

[1] SL. Kota, K. Pahlavan, and P. Leppanen, "Broadband Satellite Communications for Internet Access," Kluwer Academic Publishers: Hingham, MA, 2004.

[2] L. Zhao and J. Xie, "A novel method of scanning and tracking in satellite communication systems," IEEE Access, vol. 5, pp. 9957C9961, 2017.

[3] 3GPP TR 38.821, "Technical Specification Group Radio Access Network; Solutions for NR to Support Non-Terrestrial Networks (NTN)," 2019.

[4] F. Rinaldi, H.-L. Maattanen, J. Torsner, S. Pizzi, S. Andreev, A. Iera, Y. Koucheryavy, and G. Araniti," Non-Terrestrial Networks in 5G Beyond: A Survey," IEEE Access, vol. 8, pp. 165 178C165 200, 2020.

[5] M. Giordani, M. Polese, M. Mezzavilla, S. Rangan, and M. Zorzi, "Toward 6G Networks: Use Cases and Technologies," IEEE Communications Magazine, vol. 58, no. 3, pp. 55C61, March 2020.

[6] X. Lin, A. Adhikary, and Y.-P. Eric Wang, "Random access preamble design and detection for 3GPP narrowband IoT systems," IEEE Wireless Commun. Lett., vol. 5, no. 6, pp. 640-643, Dec. 2016.

[7] J. Zou, H. Yu, W. Miao, and C. Jiang, "Packet-based preamble design for random access in massive IoT communication systems," IEEE Access, vol. 5, pp. 11759-11767, 2017.

[8] G. Schreiber and M. Tavares, "5G new radio physical random access preamble design," in Proc. IEEE 5GWorld Forum (5GWF), Silicon Valley, CA, USA, pp. 215-220, Jul. 2018.

[9] Q. Xiong, B. Yu, C. Qian, X. Li, and C. Sun, "Random access preamble generation and procedure design for 5G-NR system," in Proc. IEEE Globecom Workshops (GC Wkshps), Abu Dhabi, United Arab Emirates, , pp. 1-7 Dec. 2018.

[10] L. Zhen, H. Qin, B. Song, R. Ding, X. Du, and M. Guizani, "Random access preamble design and detection for mobile satellite communication systems," IEEE Journals on Selected Areas in Communications, vol. 36, pp. 280C291, Feb. 2018.

[11] A. Guidotti, A. Vanelli-Coralli, M. Conti, S. Andrenacci, S. Chatzinotas, N. Maturo, B. Evans, A. Awoseyila, A. Ugolini, T. Foggi, L. Gaudio, N. Alagha, and S. Cioni, "Architectures and key technical challenges for 5G systems incorporating satellites," IEEE Trans. Veh. Technol., vol. 68, no. 3, pp. 2624-2639, Mar. 2019.

[12] H. Yizhou, C. Gaofeng, L. Pengxu, C. Ruijun, and W. Weidong, "Timing advanced estimation algorithm of low complexity based on DFT spectrum analysis for satellite system," China Commun., vol. 12, no. 4, pp. 140C150, Apr. 2015.

[13] O. Kodheli, A. Guidotti, and A. Vanelli-Coralli, "Integration of Satellites in 5G through LEO Constellations," in 2017 IEEE Global Communications Conference, pp. 1C6, 2017.

[14] X. Lin, S. Rommer, S. Euler, E. A. Yavuz, and R. S. Karlsson, "5G from Space: An Overview of 3GPP Non-Terrestrial Networks," IEEE Communications Standards Magazine, vol. 5, no. 4, pp. 147-153, Dec. 2021.

[15] M. L. Psiaki and T. E. Humphreys, "GNSS spoofing and detection," Proceedings of the IEEE, vol. 104, no. 6, pp. 1258-1270, June 2016.

[16] H. Saarnisaari, A. O. Laiyemo, and C. H. M. de Lima, "Random Access Process Analysis of 5G New Radio Based Satellite Links," in 2019 IEEE 2nd 5G World Forum (5GWF), pp. 654C658, 2019.

[17] A. Guidotti, A. Vanelli-Coralli, M. Conti, S. Andrenacci, S. Chatzinotas, N. Maturo, B. Evans, A. Awoseyila, A. Ugolini, T. Foggi, L. Gaudio, N. Alagha, and S. Cioni, "Architectures and Key Technical Challenges for 5G Systems Incorporating Satellites," IEEE Transactions on Vehicular Technology, vol. 68, no. 3, pp. 2624C2639, 2019.

[18] G. Cui, Y. He, P. Li, and W. Wang, "Enhanced timing advanced estimation with symmetric ZadoffCChu sequences for satellite systems," IEEE Communication Letter, vol. 19, no. 5, pp. 747C750, May 2015.

[19] J. J. van de Beek, M. Sandell and P. O. Borjesson, "ML estimation of time and frequency offset in OFDM systems," IEEE Transactions on Signal Processing, vol. 45, no. 7, pp. 1800-1805, July 1997.

[20] Y. Yao and G. B. Giannakis, "Blind carrier frequency offset estimation in SISO, MIMO, and multiuser OFDM systems," IEEE Transactions on Communications, vol. 53, no. 1, pp. 173-183, Jan. 2005.
[21] W. Zhou and W. H. Lam, "A novel method of Doppler shift estimation for OFDM systems," IEEE Military Communications Conference, pp. 1-7, 2008.
[22] L. Zheng and X. Wang,"Super-resolution delay-Doppler estimation for OFDM passive radar," IEEE Transactions on Signal Processing, vol. 65, no. 9, pp. 2197-2210, May 2017.
[23] H. Yizhou, C. Gaofeng, L. Pengxu, C. Ruijun, and W.Weidong, "Random access preamble design based on time pre-compensation for LTE-satellite system," J. China Univ. Posts Telecommun., vol. 22, no. 3, pp. 64-73, Jun. 2015.
[24] S. Shinakov, "Ambiguity Functions of Zadoff-Chu Signals for 5-G Synchronization Systems," 2018 Systems of Signal Synchronization, pp. 1-7, 2018.
[25] 3GPP TS 38.104, "3rd Generation Partnership Project; Technical Specification Group Radio Access Network; NR; Base Station (BS) radio transmission and reception(Release 16)," 2020.
[26] 3GPP TS 38.211, "3rd Generation Partnership Project; Technical Specification Group Radio Access Network; NR; Physical channels and modulation (Release 16)," 2020.
[27] M. Abramowitz and I. A. Stegun, Handbook of Mathematical Functions with Formulas, Graphs, and Mathematical Tables, 9th ed. New York, NY: Dover Publications, 1970.